CHIN.PHYS.LETT. Vol. 25, No. 9 (2008) 3334

Band Gap Energies and Refractive Indices of Epitaxial $Pb_{1-x}Sr_xTe$ Thin Films *

WENG Bin-Bin(翁斌斌), WU Hui-Zhen(吴惠桢)**, SI Jian-Xiao(斯剑霄), XU Tian-Ning(徐天宁)
Department of Physics, Zhejiang University, Hangzhou 310027

(Received 30 January 2008)

$Pb_{1-x}Sr_xTe$ thin films with different strontium (Sr) compositions are grown on BaF_2(111) substrates by molecular beam epitaxy (MBE). Using high resolution x-ray diffraction (HRXRD), we obtain $Pb_{1-x}Sr_xTe$ lattice constants, which vary in the range 6.462–6.492 Å. According to the Vegard law and HRXRD data, Sr compositions in $Pb_{1-x}Sr_xTe$ thin films range from 0.0–8.0%. The $Pb_{1-x}Sr_xTe$ refractive index dispersions are attained from infrared transmission spectrum characterized by Fourier transform infrared (FTIR) transmission spectroscopy. It is found that refractive index decreases while Sr content increases in $Pb_{1-x}Sr_xTe$. We also simulate the $Pb_{1-x}Sr_xTe$ transmission spectra theoretically to obtain the optical band gap energies which range between 0.320 eV and 0.449 eV. The simulated results are in good agreement with the FTIR data. Finally, we determine the relation between $Pb_{1-x}Sr_xTe$ band gap energies and Sr compositions ($E_g = 0.320+0.510x-0.930x^2+184x^3$ (eV)).

PACS: 61. 05. Cp, 78. 20. −e, 78. 30. Fs, 78. 20. Ci

Ⅳ-Ⅵ group lead-salt semiconductors, such as PbS, PbSe, PbTe and ternary semiconductor $Pb_{1-x}Sr_xTe$ and $Pb_{1-x}Sr_xSe$, have drawn considerable attention in applications of opto-electronic devices, including mid-infrared (3–30 μm) laser diodes and detectors,[1,2] due to their unique characteristics such as the direct narrow band gap at L-point of the Brillouin zone, positive temperature coefficient ($dE_g/dT > 0$), high dielectric constant, low Auger combination, distinguished thermo-electrical performance and so on.[3−5] Nowadays, the basic electronic and optical properties have been well investigated for $Pb_{1-x}Sr_xSe$.[8] These properties have been used for the growth of quantum wells and distributed Bragg reflectors (DBR) for vertical cavity surface emitting laser diodes (VCSELs) and detectors.[6,7] However, the electronic and optical properties of $Pb_{1-x}Sr_xTe$ materials that are as important as $Pb_{1-x}Sr_xSe$ have not been investigated well yet. In this study, we try to determine the electronic and optical properties of ternary compound film $Pb_{1-x}Sr_xTe$ with Sr compositions x ranging from 0.00 to 0.08. PbTe is known as a narrow band gap material with the band gap energy about 0.32 eV at room temperature (RT). SrTe, on the contrary, is a wide band gap material, which has the band gap energy above 4 eV.[9] Thus, the band gap energies of $Pb_{1-x}Sr_xTe$ are expected to increase rapidly with the addition of Sr elements.

In this work, we grew $Pb_{1-x}Sr_xTe$ thin films with different strontium (Sr) compositions x on BaF_2 (111) substrates by molecular beam epitaxy (MBE). Optical properties of the ternary thin films were studied by Fourier transform infrared (FTIR) transmission spectroscopy and the relationship between $Pb_{1-x}Sr_xTe$ band gap energies and Sr compositions was obtained. We also experimentally determined the relation between refractive index and wavelength, and have theoretically simulated transmission spectra.

$Pb_{1-x}Sr_xTe$ thin films were grown by a Ⅳ-Ⅵ group MBE system in our lab, with five different Sr compositions x ranging from 0.0% to 8.0%. PbTe compound source and Sr elemental source were used to grow $Pb_{1-x}Sr_xTe$ epitaxial layers on freshly cleaved BaF_2(111) substrates in the growth chamber of the MBE system. Details of the growth were described elsewhere.[10] The epitaxial layers were grown to the thicknesses in the range of 1.25–2.65 μm, which were measured from a Tencor Alpha-step profiler. A Philips X'pert high-resolution x-ray diffraction (HRXRD) spectrometer was used to measure the crystallinity of the epitaxial thin films.

Optical transmittance of the $Pb_{1-x}Sr_xTe$ epitaxial layers on BaF_2(111) substrates were measured at room temperature (RT) by Nexus 670 Fourier transform infrared transmission spectroscopy that was produced by Nicolet company. Its operating spectrum ranges from 50 cm^{-1} to 7400 cm^{-1} and the resolution is higher than 0.1 cm^{-1}. In order to obtain epitaxial layer transmission spectra with higher accuracy, the transmission spectra of BaF_2 substrates have been used to normalize the transmission spectra of $Pb_{1-x}Sr_xTe/BaF_2$.

Figure 1 shows a typical HRXRD curve of $Pb_{1-x}Sr_xTe$ grown on BaF_2 (111) substrate. We can only see the $Pb_{1-x}Sr_xTe$ and BaF_2 diffraction peaks in this figure. To calculate the crystal lattice constant, the angles of corresponding diffraction peaks are then used in the equation

$$a = \frac{\lambda \cdot \sqrt{h^2 + k^2 + l^2}}{2 \cdot \sin\theta} \quad (1)$$

*Supported by the Key Project of National Natural Science Foundation of China under Grant No 10434090.
**Email: hzwu@zju.edu.cn
© 2008 Chinese Physical Society and IOP Publishing Ltd

where λ is the wavelength of x-ray; h, k, and l are the Millen indices for the different planes of the ternary $Pb_{1-x}Sr_xTe$ which is of lead-salt structure, and θ is the angles of diffraction peaks. The Sr compositions are then determined by assuming the Vegard law that the lattice constant of $Pb_{1-x}Sr_xTe$ increases linearly with the increase of Sr composition. We obtain the relation between lattice constant (in units of Å) of $Pb_{1-x}Sr_xTe$ and Sr composition,

$$a = 6.462 + 0.38 \cdot x. \tag{2}$$

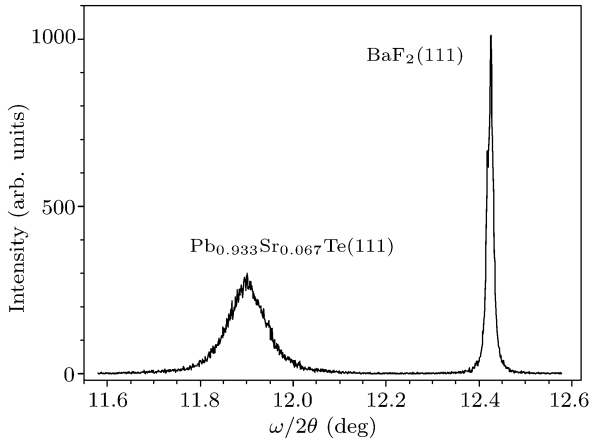

Fig. 1. High-resolution x-ray diffraction curve of the $Pb_{0.933}Sr_{0.067}Te$ thin film grown on BaF_2 (111) substrate.

Figure 2 shows FTIR transmission spectra of two $Pb_{1-x}Sr_xTe$ samples with different Sr compositions. The circles in Fig. 2 represent the measured data, which were then used to calculate the refractive indices and the absorption coefficient.

The refractive index n for each composition of Sr is determined by the interference peaks and troughs in the long wavelength λ regions with no absorption,

$$2n_m d = m\lambda_m, \quad 2n_{m+1/2}d = (m + \frac{1}{2})\lambda_{m+1/2}, \tag{3}$$

where m stands for interference peaks series, $m + 1/2$ stands for interference troughs series and d is the thickness of epitaxial layer.

The refractive index values are used for fitting the first-order Sellmeier equation[11]

$$n(\lambda) = \sqrt{1 + \frac{A_0\lambda^2}{\lambda^2 - \lambda_0^2}}, \tag{4}$$

where A_0 and λ_0 represent the fitted coefficients. Taking the $Pb_{0.939}Sr_{0.061}Te$ sample as an example, the best curve representing the change in refractive index with wavelength λ can be described by the Sellmeier equation

$$n(\lambda) = \sqrt{1 + \frac{25.284\lambda^2}{\lambda^2 - 1.277}}. \tag{5}$$

Figure 3 shows the obtained refractive indices versus wavelength for $Pb_{1-x}Sr_xTe$ with different x. It is clearly observed that the refractive index decreases while either Sr content in $Pb_{1-x}Sr_xTe$ or wavelength λ increases. We also find that the fitted curves are all matched well with the experimental data.

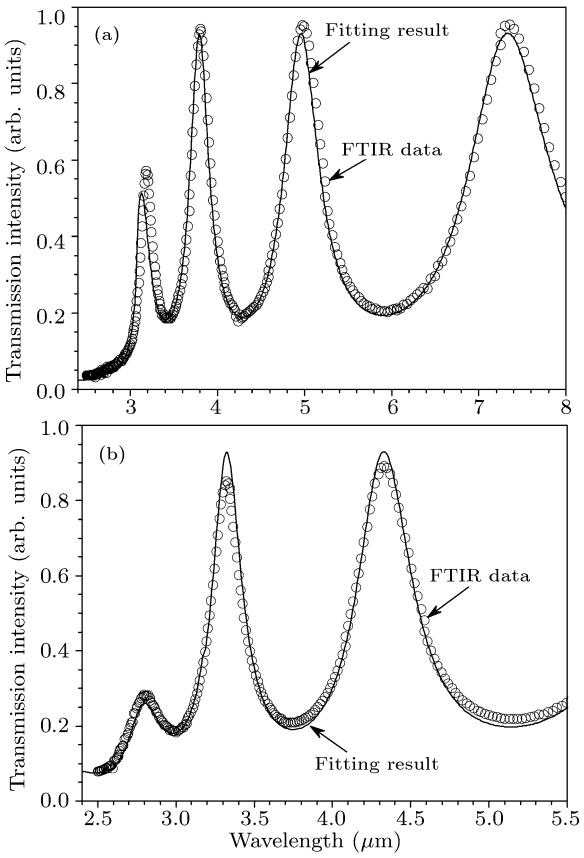

Fig. 2. Transmission spectra for two $Pb_{1-x}Sr_xTe$ samples with both experimental (FTIR) data (circles) and theoretical results (lines): (a) $Pb_{0.939}Sr_{0.061}Te$, (b) $Pb_{0.920}Sr_{0.080}Te$.

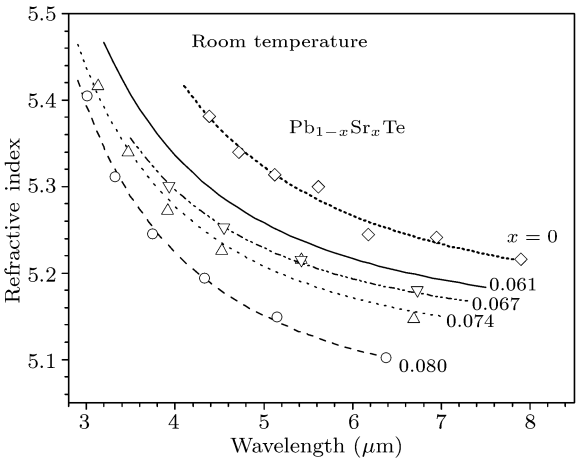

Fig. 3. Refractive indices versus infrared wavelength at room temperature for $Pb_{1-x}Sr_xTe$, the symbols are the experimental data and lines are the fitted data.

For testing whether the refractive indices we determined are correct or not and determining the energy gaps of the $Pb_{1-x}Sr_xTe$ thin films, the refractive indices obtained are then used to simulate the FTIR transmission spectra. The transmission T is a complex function given by[12]

$$T = \frac{A'x}{B' - C'x + D'x^2}, \tag{6}$$

where

$$\begin{aligned}
A' &= 16s(n^2+k^2),\\
B' &= [(n+1)^2+k^2][(n+1)(n+s^2)+k^2],\\
C' &= [(n^2-1+k^2)(n^2-s^2+k^2)\\
&\quad -2k^2(s^2+1)]2\cos\varphi - k[2(n^2-s^2+k^2)\\
&\quad +(s^2+1)(n^2-1+k^2)]2\sin\varphi\\
D' &= [(n-1)^2+k^2][(n-1)(n-s^2)+k^2],\\
\varphi &= 4\pi nd/\lambda,\ x = \exp(-\alpha d),\ \alpha = 4\pi k/\lambda,
\end{aligned}$$

where s stands for the refractive index of the substrate BaF_2, which obeys the third-order Sellmeier equation

$$s = \left[1 + \frac{0.643\lambda^2}{\lambda^2-(0.0578)^2} + \frac{0.507\lambda^2}{\lambda^2-(0.110)^2} + \frac{3.826\lambda^2}{\lambda^2-(146.386)^2}\right]^{1/2}, \tag{7}$$

in which the wavelength ranges from $0.27\,\mu$m to $10.3\,\mu$m.

Generally, the photon energy is smaller than band gap energy of the films, the photon absorption is so weak that k in Eq. (6) can be zero. When photon energy is nearly the same as or larger than the band gap energy, the absorption coefficient values are estimated to be $\alpha \approx 10^4\,\mathrm{cm}^{-1}$ and the value of k is approximately equal to 10^{-1}. However, the refractive index n of PbTe is greater that 5.0. Consequentially, it satisfies $k^2 \ll n^2$. Totally, the definition of $k = 0$ is valid in most of the transmission spectra regions. Therefore, Eq. (6) becomes much simpler, which is expressed as

$$T = \frac{Ax}{B - Cx\cos\varphi + Dx^2}, \tag{8}$$

where

$$\begin{aligned}
&A = 16n^2s, \quad B = (n+1)^3(n+s^2),\\
&C = 2(n^2-1)(n^2-s^2), \quad D = (n-1)^3(n-s^2),\\
&\varphi = 4\pi nd/\lambda, \quad x = \exp(-\alpha d)
\end{aligned}$$

We divide the transmission spectra into three regions, which are respectively transparent region, weak and medium absorption region, and strong absorption region in which interference fringes disappear.

The absorption coefficients in the three regions of transmission spectra read[12]

$$\begin{cases}
\alpha \simeq 0, \quad \text{for} \quad E_{\text{photon}} \ll E_g,\\
\alpha = -\dfrac{1}{d}\ln\left[\dfrac{F - [F^2-(n^2-1)^3(n^2-s^4)]^{1/2}}{(n-1)^3(n-s^2)}\right],\\
F = \dfrac{8n^2s}{T_i},\ T_i = \dfrac{2T_MT_m}{T_M+T_m}, \ \text{for } E_{\text{photon}} < E_g,\\
\alpha \simeq -\dfrac{1}{d}\ln\left[\dfrac{(n-1)^3(n+s^2)}{16n^2s}T_0\right], \ \text{for } E_{\text{photon}} > E_g.
\end{cases} \tag{9}$$

Adopting the obtained refractive indices, we simulate the $Pb_{1-x}Sr_xTe$ transmission spectra with the theoretical model described above. In Fig. 2, the transmission spectra with both FTIR data and theoretical fitted results for the two $Pb_{1-x}Sr_xTe$ samples are plotted. Clearly, the theoretical results are consistent with the FTIR results. Therefore, we can draw the conclusion that the refractive indices determined above can well display the optical properties of the epitaxial $Pb_{1-x}Sr_xTe$ thin films.

It is known that $Pb_{1-x}Sr_xTe$ material system with a small content of Sr(x is approximately less than 20%) has direct band gaps.[8] For this material system, the band gap energy can be extrapolated by the equation[13]

$$\alpha_{\text{direct}} = \frac{A}{(h\nu)^{1/2}}(h\nu - E_g)^{1/2}, \tag{10}$$

where α_{direct} is the absorption coefficient, A is constant, $h\nu$ is the photon energy and E_g is the band gap energy of $Pb_{1-x}Sr_xTe$. The above equation is valid only when the photon energy is equal to or greater than the band gap energy ($h\nu > E_g$). Therefore, we only use the strong absorption region for our band gap energy calculations.

According to Eq. (10), the band gap energies of the five samples are then extrapolated by fitting this absorption equation. The band gap energies obtained are listed in Table 1.

Table 1. Parameters of five $Pb_{1-x}Sr_xTe$ thin film samples.

Sample	$Pb_{1-x}Sr_xTe$ thickness (μm)	Lattice constant (Å)	Sr compositions	Band gap energy (eV) at room temperature
1	2.65	6.462	0.0%	0.320
2	1.42	6.485	6.1%	0.388
3	1.30	6.488	6.7%	0.404
4	1.30	6.490	7.4%	0.432
5	1.25	6.492	8.0%	0.449

Figure 4 shows the band gap energies of $Pb_{1-x}Sr_xTe$ for different compositions at room temperature. The best-fit curve for the calculated band gap energies (in units of eV) of $Pb_{1-x}Sr_xTe$ follows an equation of the Sr composition x as

$$E_g = 0.320 + 0.510x - 0.930x^2 + 184x^3. \qquad (11)$$

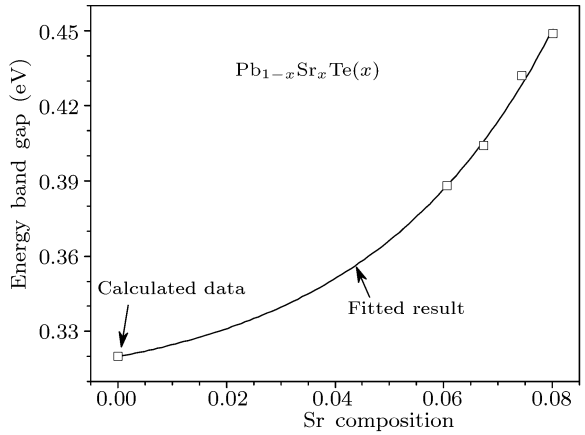

Fig. 4. Band gap energies for different Sr compositions in $Pb_{1-x}Sr_xTe$ at room temperature. Squares show the experimental data, and the line is the fitted curve.

In summary, we have realized $Pb_{1-x}Sr_xTe$ thin films with different strontium compositions using MBE and obtained the ternary material $Pb_{1-x}Sr_xTe$ crystal lattice constants versus Sr composition. The refractive indices $n(\lambda)$ of $Pb_{1-x}Sr_xTe$ with x ranging from 0.00 to 0.08 are experimentally determined. Based on the obtained refractive indices, we also simulate the $Pb_{1-x}Sr_xTe$ transmission spectra that are in good agreement with the FTIR results. By the simulation of the measured transmission spectra, the band gap energies E_g of $Pb_{1-x}Sr_xTe$ are also obtained. The data of lattice constants, refractive indices, absorption coefficients and band gap energies attained in this work are essential for further development of opto-electronic devices in this material system.

References

[1] Chao I N, McCann P J, Yuan W L, O'Rear E A and Yuan S 1998 *Thin Solid Films* **323** 126
[2] Kellermann K, Zimin D, Alchalabi K, Gasser P, Pikhtin N A and Zogg H 2003 *J. Appl. Phys.* **94** 7053
[3] Wang Q L, Wu H Z, Si J X, Xu T N, Xia M L, Xie Z S and Lao Y F 2007 *Acta Phys. Sin.* **56** 4950 (in Chinese)
[4] Xu T N, Wu H Z, Si J X and McCann P J 2007 *Phys. Rev.* B **76** 155328
[5] Wu H Z, Cao C F, Si J X, Xu T N, Zhang H J, Wu H F, Chen J, Shen W Z and Dai N 2007 *J. Appl. Phys.* **101** 103505
[6] Shi Z, Xu G, McCann P J, Fang X M, Dai N, Felix C L, Bewley W W, Vurgaftman I and Meyer J R 2000 *Appl. Phys. Lett.* **76** 3688
[7] Wu H, Zhao F, Jayasinghe L and Shi Z 2002 *J. Vac. Sci. Technol.* B **20** 1356
[8] Majumdar A, Xu H Z, Zhao F, Keay J C, Jayasinghe L, Khosravani S, Lu X, Kelkar V and Shi Z 2004 *J. Appl. Phys.* **95** 939
[9] Partin D L, Thrush C M and Clemens B M 1986 *J. Vac. Sci. Thechnol.* B **5** 687
[10] Si J X, Wu H Z, Xu T N, Cao C F, Huang Z C 2005 *Chin. Phys. Lett.* **22** 2352
[11] Tatian B 1984 *Appl. Opt.* **23** 4477
[12] Swanepoel R 1983 *J. Phys. E: Sci. Instrum.* **16** 1214
[13] Diaz R, Merino J M, Martin T, Rueda F and Leon M 1998 *J. Appl. Phys.* **83** 616